Heat-Dependent Hairpin Melting Drives TRPV1 Opening

Guangyu Wang*

Department of Physiology and Membrane Biology, University of California School of Medicine, Davis, CA, USA

Department of Drug Research and Development, Institute of Biophysical Medico-chemistry, Reno, NV, USA

* Author to whom correspondence should be addressed; E-mail: gary.wang10@gmail.com

Abstract

The capsaicin receptor TRPV1 is a bio-thermometer in a primary afferent sensory neuron for noxious heat detection. However, the underlying molecular mechanism is unclear. Here, a hairpin thermodynamic model, together with graph theory, was used to examine a role of temperature-dependent little hairpin sizes in controlling the temperature threshold and sensitivity and gating states of TRPV1. The results showed that heat-evoked melting of the biggest little hairpin with a minimum loop size initiates a temperature threshold for channel opening while the smaller hairpins with strong H-bonds may stabilize the open state and increase the heat efficacy. The temperature sensitivity is determined by a change of the total minimum sizes of little hairpins upon a change of the total non-covalent interactions along the gating pathway from a closed state to an open one. Therefore, this model may provide a broad structural basis for the thermo-gated TRP channels. (146 words)

Running title: Digital codes in heat-sensing TRPV1

Keywords: desensitization; gating loop; graph theory; hairpin thermodynamics; ion channel; non-covalent interaction; temperature sensitivity; threshold

1. INTRODUCTION

Temperature is important in everyday life. Transient receptor potential (TRP) vanilloid-1 (TRPV1) is well-known as a noxious heat sensor in a primary afferent neuron of the dorsal root and the trigeminal ganglia. Its activation allows sodium or calcium to be permeable to a channel pore. With a temperature activation threshold (~42°C) above a normal human body temperature 37°C and a temperature coefficient Q_{10} (defined as the ratio of equilibrium constants measured 10°C apart) higher than 20, this channel can work as a bio-thermometer to monitor any noxious heat signal above 42°C and to regulate the human body temperature. [1-4] In addition to the physical stimuli, capsaicin can also activate TRPV1, producing hot sensation. As cold can decrease the capsaicin-evoked activity of TRPV1, [5] the same gating pathway seems to be shared by both stimuli. On the other hand, residues sensitive to both physical and chemical stimuli are different in TRPV1, suggesting their different gating pathways. [6-9]

TRPV1 is a homotetramer with each monomer consisting of six transmembrane helices. The first four segments (S1–S4) form a voltage-sensor-like domain (VSLD) while the last two (S5 and S6), together with the intervening loop and the pore helix and the extracellular cap-like pore turret between S5 and S6, are folded as a pore domain. The pore domain is surrounded by the VSLD in a domain-swapped arrangement. The cation conductance pathway centers in the pore domain. A hydrophobic constriction around I697 forms a lower S6 gate while the segment from G643 to D646 (^{643}GMGD^{646}) between S5 and S6 (S5-P-S6) in rat TRPV1 (rTRPV1) acts as a short selectivity filter. The S4–S5 linker, which is a short amphipathic helix and almost parallel to the cytoplasmic membrane, couples the VSLD with the pore domain for channel gating. Thus, the overall structure of the TRPV1 channel resembles that of the voltage-gated ion channel. [10-11] However, TRPV1 has a conserved TRP domain, which runs parallel to the inner leaflet of the membrane by virtue of a sharp bend after S6, not only linking the S6 gate crossing bundle but also interacting with the S4–S5 linker and the pre-S1 domain in favor of allosteric coupling between different gating domains. In addition, the characteristic ankyrin repeats within the cytoplasmic N terminus can tether cytoplasmic N- and C-terminal domains for channel assembly. [11-14] Although the structural basis for the chemical stimuli such as capsaicin has been clear, [15-16] the heat-evoked gating pathway is still unknown for TRPV1 regarding the temperature threshold and sensitivity and desensitization.

Since 2013 a DNA hairpin thermal sensor with a limited poly-A loop size has been created to monitor a change in a biological microenvironment. [17] Its initial hairpin melting curve is similar to the temperature-dependent activation curve of the thermosensitive TRPV channels. Its hairpin melting temperatures are also in a threshold range of thermosensitive TRPV channels despite an increase with the smaller or less-flexible loop, the shorter duplexed stem, the more H-bonding pairs at the ends, or the higher ionic strength in an aqueous solution. [1, 6, 18-23] In this regard, it is fitting to ask if the thermosensitive TRPV channels exploit a series of little hairpins with minimum loop sizes to control the temperature thresholds and sensitivity or Q_{10} and gating states. In this study, graph theory was used as a novel tool to examine this hypothesis by analyzing the cryo-electron microscopy (cryo-EM) structural data of rTRPV1 with or without phosphatidylinositol (PI)-bound at the capsaicin site around the temperature threshold. This hairpin thermodynamic model generates several melting temperatures (T_m) and structural thermo-sensitivity (Ω_{10}) values which are comparable to the experimental thresholds (Tth) and functional thermo-sensitivity Q_{10} values, respectively. Therefore, these results are consistent with the proposals that the melting temperature of the biggest little hairpin with a minimum loop size in rTRPV1 may be responsible for the temperature threshold for channel activation, and that Q_{10} may be controlled by a change of the total minimum loop sizes of the little hairpins in response to a change of the total non-covalent interactions along the gating pathway from a closed state to an open one with 10°C apart.

2. RESULTS

2.1. The PI-free rTRPV1 Had the First Biggest Little Hairpin in the VSLD at 4°C

When capsain competes off the PI lipid at low and high temperatures, this vanilloid compound did not not bridge any two aminop acid chains in rTRPV1 to cause any little hairpin in the presence of MSP2N2 under the given nanodisc condition. [14] Therefore, the state-dependent cryo-EM structures of PI-free rTRPV1 at different temperatures could be used to examine the role of temperature-dependent little hairpin melting in the gating pathway. At 4°C, several kinds of non-covalent interactions between amino acid side chains along the gating pathway from D388 in the pre-S1 domain to K710 in the TRP domain formed a little hairpin topological loop network in the closed state.

First, salt bridges between pairwise charged residues were required to shape little hairpins. They included K425-E709 in the pre-S1/TRP interface, D427-K431 in the pre-S1/VSLD interface,

D471-R474 on S2, R534-E536 in the S3-S4 linker, E570-K571 in the S4-S5 linker, E636-K639 on the pore helix (**Fig. 1A**).

Second, π interactions involving aromatic side rings also brought about little hairpins. In the VSLD and its interfaces with the pre-S1 domain and TRP domain and the S4-S5 linker, these π-interacting pairs covered Y401-E397/R499, H410-I696, W426/W697-R701, F434-W426/Y555, F438-Y555, Y441-F488/F516/Y555, Y444-F448/F488, M445-W549, Y453-Y454, V486-F490, Y487-F488, F488-F516, F489-I493/L524, Y495-R499/E513, F507-I514, F516-N551/Y554, F517-L521, F522-F543, Y530-F531/Y537, and Y554-Y555/R557. In the pore domain, the π-interacting pairs had F580-F584/L678, F589-T593, F591-Y666, Y627/E636-F649, F640-Y666, F659-Y653/F649/L663, and Y666-T670 (**Fig. 1A**).

Third, H-bonds between different hydrophilic amino acid side chains also contributed to the formation of little hairpins. In the VSLD and its interfaces with the TRP domain and pre-S1 domain or the S4-S5 linker, these H-bonding pairs were Y401-D707, D411-N695, Q423-D427/R701, D424-R428, Y441/N551-Q519, T449-W549, Y463/Y537-K535, Y487-R491, Q494-Q498, and R557-Q700. In the pore domain and its interface with the TRP domain, the H-bonding pairs included D576-R579/T685, Y584-T641/Y666, T641-Y666, and Q691-N695 (**Fig. 1A**).

Taken together, along the gating pathway from D388 to K710, sixty seven non-covalent interactions produced the total number of minimum hairpin sizes as 119 (**Fig 1A**). Among the multiple little hairpins, although several smaller ones had 0 to 8 minimum residues in the loops, the biggest one was outstanding in the VSLD. It had a minimum 24-residue loop from T449 to Y463, K535, Y537 and W549 and back to T449 to control the Y463-K535 H-bond (**Fig.1B-C**). Because one and half equivalent H-bonds formed this little hairpin loop, the predicted melting temperature was 21°C (**Table 1**).

2.2. The Second Biggest Little Hairpin Appeared in the VSLD/pre-S1/TRP/VSLD interfaces at 25°C

If the first biggest little hairpin with a minimum 24-residue loop in rTRPV1 carries out the single-step melting reaction like DNA hairpins, the calculated melting temperature 21°C should be enough to open it or to change its size above 21°C (**Table 1**). In agreement with this assumption, when the temperature raised from 4°C to 25°C, a new R455-Y537 H-bond was born so that the Y463-K535 H-bond could be controlled by a smaller little hairpin with a minimum 7-residue loop

(Fig. 2A-B, D). This change rearranged some non-covalent interactions along the gating pathway (Fig.2A).

Table 1 New parameters of the rTRPV1 bio-thermometer based on the hairpin thermodynamic model

Construct	**Control**	**rTRPV1**				
Lipid environment	MSP2N2	MSP2N2				native
PDB ID	7LPE	7LPA	7LPB	7LPD	7LPC	7LPC
Lipid PI	free	free	free	free	bound	bound
Sampling temperature	**48°C**	**4°C**	**25°C**	**48°C**	**48°C**	
Gating state	open	closed	closed	inactivated	closed	closed
# of the biggest little hairpin	3	1	2	4	6	5
Biggest little loop size (L_{max}), a.a	12	24	10	7	12	16
Equivalent H-bonds in L_{max}	2	1.5	1	2	2.5	2
Total non-covalent interactions	63	67	77	67	77	75
Total little hairpin sizes, a.a.	97	119	121	79	116	128
Calculated melting temperature	50°C	**21°C**	**44°C**	60°C	**55°C**	**42°C**
Measured threshold T_{th}		**<25°C**	**<48°C**		**>48°C**	**42°C**
Calculated $\Omega_{10,\ min}$			8.90		6.69	11.4
Calculated $\Omega_{10,\ mean}$			**20.7**		**15.6**	**26.1**
Calculated $\Omega_{10,\ max}$			79.2		59.6	96.4
Measured Q_{10}			**16.4**			**21.9-26**
Ref. for T_{th} and Q_{10}			[14]			[1, 14]

Note: E=0.5, 1, 3 kJ/mol for the minimum, mean and maximal intensity of a non-covalent interaction in the hairpin loop.

In the VSLD, the Q494-Q498 H-bond, the F507-E513 π interaction were broken while the K466-D471 and R491-E513 salt bridges, the S505-D509 H-bond, and the Y495-F496 and Y511-L515 π interactions were added. In the meanwhile, the H-bond and the π interaction exchanged in the Y487-R491 and Y495-R499 pairs. In the VSLD/pre-S1 interface, the salt bridge shifted from the D427-K431 pair to the R409-D509 pair. In the VSLD/TRP interface, R491 formed a salt

bridge with D707. As a result, in the pre-S1/TRP interface, the H410-I696 π interaction and the D411-N695 H-bond were disconnected. In the S4-S5 linker/TRP interface, the R557-T704 and Q560-K694 H-bonds were present. In the pore domain and its interfaces with the S4-S5 linker and the TRP domain, the new non-covalent interactions included the E648-K656 and K688-E692 salt bridges and the T650-N652 H-bond. This global conformational change demonstrated that the pore domain was coupled to the VSLD via the interaction between the S4-S5 linker and the TRP domain.

Along the gating pathway from D388 to K710, although the total number of all minimum hairpin loop sizes slightly increased from 119 to 121, the total number of all non-covalent interactions significantly raised from 67 to 77 (**Fig.2A**). When the R409-D509 and R491-E513/D707 salt bridges and the Y401-D707 H-bond in the interfaces of the VSLD with the pre-S1 domain and the TRP domain generated the second biggest little hairpin with a minimum 10-residue loop from Y401 to R409 and D509 and E513 and R491 and back to Y401 (**Fig. 2C-D**), one equivalent H-bond produced a melting temperature 44°C based on the single-step melting reaction like DNA hairpins (**Table 1**).

2.3. rTRPV1 Opened at 48°C with High Q_{10} in the Absence of the Second Biggest Little Hairpin in the TRP/VSLD/pre-S1 Interfaces but Presence of the Third One in the VSLD/S4-S5 Linker Interface

When PI-free rTRPV1 opened at 48°C upon the melting of the second biggest little hairpin with a minimum 10-residue loop in the TRP/VSLD/pre-S1 interfaces, several changes occurred in non-covalent interactions (**Fig. 3A**).

The R409-D509 and R491-E513/D707 and E397-K710 and K425-E709 salt bridges and the Q423-D427/R701 and D424-R428 H-bonds and the E397-Y401 π interaction were broken. In the meantime, in the presence of the Y401-R499 π interaction, Y401 formed a new H-bond with Q498 so that a smallest little hairpin with no residue in the loop bridged the VSLD with the pre-S1 domain. When the Y554-R557 π interaction was disrupted, Y554 also generated an H-bond with T704 to stabilize the S4-S5 linker/TRP interface together with the R557-Q700 H-bond. As a result, in the VSLD/S4-S5 linker interface, the π interaction moved from Y555-F438 to F559-F434/F438 with the formation of the R557-E570 H-bond.

When this conformational change extended to the VSLD, the D471-K466/R474 and R534-E536 salt bridges, the S505-D509 and K535-Y463/Y537 and Q519-Y441/N551 H-bonds, and the

Y441-F488 and Y530-F531 π interactions were disconnected. In the meanwhile, the new Y495-S510 H-bond and the new R499-D509 salt bridge and the new F448-S481 and Y454-R474 π interactions emerged.

When this conformational change extended to the pore domain and its interfaces with the S4-S5 linker and the TRP domain, the Q560-K694 and D576-R579 and Q691-N695 H-bonds, the E570-K571 and E648-K656 and K688-E692 salt bridges, and the Y627-F649 π–π interaction were disrupted. In the meanwhile, the new D601-N628/N652 and Y653-K653 H-bonds and the E651-K656 salt bridge were born.

By all accounts, the total numbers of all non-covalent interactions and minimum hairpin sizes along the gating pathway from D388 to K710 dramatically decreased from 77 and 121 to 63 and 97, respectively (Fig. 3A). As a result, the structural thermo-sensitivity Ω_{10} was about 20.2, which was similar to the experimental Q_{10} value (~16.4). [14] On the other hand, the R557-E570 bridge had two equivalent H-bonds in this third biggest little hairpin so that the melting temperature was as high as 50°C (**Fig. 3C, Table 1**).

2.4. rTRPV1 Inactivated at 48°C with the Fourth Biggest Little Hairpin in the VSLD

When E570 in the S4-S5 linker further formed an H-bond with Q700 in the TRP domain at 48°C, the third biggest little hairpin in the open state disappeared with other changes (**Fig. 4A-B**). In the pre-S1/TRP/pore domain interface, the Y401-D707 H-bond was replaced with H410-E692 π interaction and the N695-H410/Q691 H-bonds. As a result, in the interface between the pore domain and the S4-S5 linker, the E570-K571 salt bridge and the D576-R579 H-bond were reinstated. In the outer pore, the D601-N628/N652 and T650-N652 and Y653-K656 H-bonds were disconnected. In the meanwhile, the E651-K656 salt bridge became an H-bond and the Y627-F649/E636 π interactions were present. When the F559-F434/F438 π interactions were broken in the S4-S5 linker/VSLD interface, the Y401-Q498 H-bond was disrupted in the pre-S1/VSLD interface. In the meanwhile, the E397-Y401 π interaction was restored with the new R420-Q423 H-bond in the pre-S1 domain. Finally, in the VSLD, the F448-S481 and Y454-R474 and Y495-F496 and F517-F496/L521 π interactions were broken with the R499-D509 salt bridge. In the meanwhile, the F438-Y555 and Y444-F488 and F489-L524 and Y530-F531 and Y554-Y555 π interactions and the Y464-K535 and Q494-Q498 and R534-E536 H-bonds were restored with the new Y463-Y537 and R491-Q494 H-bonds.

Taken together, although the total number of all non-covalent interactions along the gating pathway from D388 to K710 slightly increased from 63 to 67, the total number of the minimum hairpin loop sizes significantly decreased from 97 to 79 residues (Fig 4A). In other words, this state was much more stable than the open state and thus served as an inactivated state to desensitize the channel activity. The fourth biggest little hairpin with a minimum 7-residue loop also appeared in the VSLD. It started with R455 and through Y537 and ended with Y463 (**Fig. 4C-D**). The resultant melting temperature was about 60°C (**Table 1**).

2.5. The Replacement of the Fifth Biggest little Hairpin in the VSLD/pre-S1 Interface with the Sixth One in the VSLD Prevented the PI-bound rTRPV1 in MSP2N2 from Opening at 48°C

When the resident PI occupies the well-known vanilloid site, rTRPV1 in MSP2N2 cannot open even at 48°C. This closed state of PI-bound rTRPV1 is almost identical between 4°C and 48°C. [14] However, compared to PI-free rTRPV1 at 25°C, there were several differences once the PI lipid linked R409, D509, R557, E570 and Q700 together via H-bonds (**Fig. 5A-B**).

In the pore domain and its interfaces with the S4-S5 linker and the TRP domain, the E648-K656 and K688-E692 salt bridges and the T650-N652 H-bond were disrupted with the formation of the Y627-E636 and E692-K571/R575 hydrogen or salt bridges and the F587-F591 and D654-F655 π interactions. In the VSLD, the K466-D471 and R491-E513 salt bridges, the R455-Y537 and Y495-R499 and S505-D509 and K535-Y537 H-bonds, and the Y495-F496 and Y511-L515 π interactions were disrupted. In the meanwhile, the Y463-Y537 H-bond and the F489-F490 π interaction were formed with the shift of the π interaction from F496-F517 to Y495-E513. In addition, both the R474-D471 salt bridge and the Y487-R491 π interaction became the H-bonds.

When the H-bond shifted from R557-T704 to Y554-T704 pairs in the VSLD/TRP interface, the salt bridge also moved from R491-D707 to R499-D707 in the VSLD/TRP interface. In this case, although the smallest little hairpin with no residue in the loop could control the Y401-R499 π interaction and the R499-D707 salt bridge and the D707-Y401 H-bond, the fifth biggest little hairpin with a minimum 16-residue loop from Y401 to R409 and D509 and R409 and back to Y401 should provide a melting temperature 42°C as a threshold to release the PI lipid from the vanilloid site for rTRPV1 opening (**Table 1, Fig. 5A, C, E**). Even if the E397-Y401 and the D424-R428 H-bond were disconnected in the VSLD/pre-S1 interface, the total number of the non-covalent interactions and minimum hairpin loop sizes along the gating pathway would be 75 and

128. If the same open state was employed, the structural thermo-sensitivity Ω_{10} would be about 26.1, which was comparable to the Q10 value (21.9-26) (**Table 1**). [1, 14]

However, rTRPV1 in MSP2N2 allowed H410 in the pre-S1 domain to form an H-bond and a π interaction with N695 and I696 in the TRP domain, respectively. In that case, the sixth biggest little hairpin was present in the VSLD. It had a minimum 12-residue loop from D509 to F516, Y554 and R557 and back to D509 via the PI lipid (**Fig.5A, D, E**). If that sixth biggest little hairpin was also subjective to the single-step melting reaction like the DNA hairpin, the melting temperature was as high as 55°C. That may be why the PI-bound rTRPV1 in MSP2N2 cannot open at 48°C. [14] Of special note, the decrease of the total minimum hairpin loop sizes from 128 to 116 also resulted in a decrease in the structural thermo-sensitivity Ω_{10} from 26.1 to 15.6 for rTRPV1 in such a tight lipid environment (**Table 1**).

3. DISCUSSION

TRPV1 is designed and created as a bio-thermometer in the thermostable system to detect noxious heat and to protect a human or animal body from heat damage. [1-4] To this end, it should meet several protein engineering requirements. First, it should be an integral membrane protein with a relative high physicochemical stability or heat capacity to avoid thermal denaturation. Second, it should be an ion channel that can directly couple a temperature signal to an electronical signal reporter for a readout by a primary afferent sensory neuron. Third, its opening from the closed state within 10°C apart should have a high Q_{10} with a steep response to a small change in a surround predetermined temperature. Fourth, it should have a heat switch with two temperature threshold limits for two gating states, one for activation to sense noxious heat and the other for inactivation to alleviate pain by exploiting use-dependent desensitization upon constant noxious heat stimuli. In the biological and chemical world, a hairpin topological loop structure may be an ideal tool for thermosensitive TRP channels to achieve them.

The DNA hairpin with the limited loop sizes has been designed as a temperature switch, a thermometer and an ionic detector with Q_{10} in the range from 1.8 to 2.7. Its oligonucleotides with complementary nucleotide sequences at the ends form a duplex region as the hairpin stem upon intra-strand hybridization, and its nucleotides in between as the hairpin loop. When a temperature increases above a threshold, the DNA hairpin melts and thus becomes single stranded. Its melting temperature threshold sharply depends on the H-bonded base pairs in the stem, the size and flexibility of the loop and the ionic strength in a solution. Generally, a stable stem or a small and

rigid loop or a high salt concentration in the solution allows the DNA hairpin to have a high threshold to sense and to respond to highly specific and small changes in an environmental temperature. When the loop length is decreased from 20 to 10 A's or the H-bonded G-C base-pairs raise from 2 to 4, the melting temperature threshold can be increased more than 20 degrees. Clearly, a short stem favors sharp hairpin melting rather than gradual melting. Since a change in the loop sequence has no significant effect on the melting temperature threshold of the DNA biosensor, [17] once noncovalent interactions create a hairpin topological loop, the hairpin thermodynamics should be comparable between DNA and protein.

Like the DNA hairpin thermal biosensor, at a given physiological salt concentration (150 mM NaCl), when non-covalent interactions made the biggest little hairpin with a minimum loop size along the gating pathway from D388 in the pre-S1 domain to K710 in rTRPV1, the melting temperature increased with a decreased loop size and an increased number of equivalent H-bonds in the loop. In the absence of the PI lipid at the vanilloid site, rTRPV1 had the first biggest little hairpin with a minimum 24-residue loop from T449 to Y537 and K535 and Y463 and back to T449 in the VSLD to control the Y463-K535 H-bond at 4°C (**Fig. 1**). One and half equivalent H-bonds in the loop allowed the melting temperature to be about 21°C (**Table 1**). However, the Y463-K535 H-bond was not broken at 25°C. Instead, Y537 formed another H-bond with R455, decreasing the minimum loop size from 24 to 7 residues to hold the Y463-K535 H-bond. As a result, the second biggest little hairpin was born with a minimum 10-residue loop from Y401 to R409, D509, E513, R491 and D707 to control the R409-D509 salt bridge (**Fig. 2**). As one equivalent H-bond kept this loop, the melting temperature was about 44°C (**Table 1**). Therefore, its melting at 48°C further disrupted three salt bridges in the loop and resulted in the formation of the third biggest little hairpin with a minimum 12-residue loop from R557 to E570 (**Fig. 3**). However, the presence of two equivalent H-bonds to control the R557-E570 bridge set a melting temperature threshold at about 50°C (**Table 1**). Therefore, at 48°C the formation of the E570-Q700 H-bond generated the smallest little hairpin with no residue in the loop to increase the melting temperature up to about 74°C via two equivalent H-bonds in the loop. In this case, the fourth biggest little hairpin appeared in the VSLD with a minimum 7-residue loop from R455 to Y537 and Y463 and back to R455 (**Fig.4**). This loop had two equivalent H-bonds so that the melting temperature was about 60°C (**Table 1**). On the other hand, in the absence of the H410-I696/N695 bridge in a native lipid environment, no matter whether PI was present at the capsaicin

site or not, the fifth biggest little hairpin would have a normal melting temperature 42°C in the presence of two equivalent H-bonds in a minimum 16-residue loop from Y401 to R409 and D509 and R499 and back to Y401 (**Table 1, Fig. 5A, B, C, E**). However, once PI-bound rTRPV1 was reconstituted in MSP2N2, the presence of the H410-I696/N695 bridge allowed the sixth biggest little hairpin in the VSLD to have 2.5 equivalent H-bonds to maintain a minimum 12-residue loop from D509 to F516 and Y554 and R557 and back to D509 via the PI lipid bridge. The resultant melting temperature 55°C could prevent the D509-PI-R557 bridge from melting at 48°C for channel opening (**Table 1, Fig. 5A, B, D, E**). Therefore, like a DNA hairpin, a single-step melting reaction of the biggest little hairpin topological loop may be enough to initiate the temperature-dependent threshold in rTRPV1.

Despite six biggest little hairpins in rTRPV1, their roles in gating states may be different. The additional R455-Y537 H-bond decreased the loop size of the first biggest little hairpin from 24 to 7 residues to hold the Y463-K535 H-bond above 21°C. All these happened in the VSLD so that the channel was still closed (**Table 1, Fig. 1-2**). In stark contrast, the second one was closely coupled to the lower S6 gate via the R409-D509 salt bridge in the VSLD/pre-S1 interface and the R491-D707 salt bridge in the VSLD/TRP interface. Therefore, its melting disrupted these two salt bridges, allowing PI-free rTRPV1 to open above 44°C (**Table 1, Figs. 2-3**). Although the third biggest little hairpin may favor the open state by uplifting the S4-S5 linker against the S6 gate via the stimulatory R557-E570 H-bond in the VSLD/S4-S5 linker interface, it had an upper melting temperature limit 50°C. Accordingly, when another E570-Q700 H-bond decreased the minimum loop size from 12 residues to zero for a higher melting temperature 74°C to protect the R557-E570 from the disruption above 50°C, the fourth biggest little hairpin appeared between the S1-S2 linker and the S3-S4 linker to govern the inactivated state, alleviating pain upon constant noxious heat stimuli-induced desensitization (**Table 1, Figs. 3-4**). [1, 8, 14, 24] In fact, platypus (*Ornithorhynchus anatinus*) TRPV1 (pTRPV1) has no inactivation possibly with different amino acid sequences in both linkers to damage this biggest little hairpin in the VSLD [24]. Since the fourth biggest little hairpin factually had the melting temperature 60°C (**Table 1**), the upper threshold limit for the rTRPV1 bio-thermometer may be 60°C. In the native lipid system, the fifth putative biggest little hairpin with a minimum 16-residue loop in the VSLD/pre-S1 interface may have a normal melting temperature 42°C (**Table 1, Fig. 5C, E**). Like the second one, its melting above 42°C may disrupt the R409-D509 salt bridge in favor of channel opening. When the salt concentration was lowered

down from 150 mM to 130 mM, the threshold may also decrease from 42°C to 37.7°C. [8] On the other hand, when rTRPV1 was reconstituted in MSP2N2, the sixth biggest little hairpin had a minimum 12-residue loop in the VSLD to control the D509-PI-R557 bridge. Its very high melting temperature 55°C may be beyond the physiological range for the detection of noxious heat unless a vanilloid compound like capsaicin could bind near D509 and R557 to remove the PI lipid (**Table 1, Fig. 5D, E**). [14] Taking all these into account, the channel opening may be initiated by inter-domain interactions in a thermometer range from 42°C to 60°C to monitor the noxious heat. Further experiments are necessary to examine the role of the Y401-R499 π interaction and the R409-D509 salt bridge in securing the normal temperature threshold 42°C for rTRPV1 opening.

When PI-free rTRPV1 opens at 48°C from a closed state at 25°C, the opening of multiple little hairpins may increase entropy but decrease enthalpy as a result of the decrease in the total non-covalent interactions from 77 to 63 along the gating pathway from D388 to K710 (Figs 2-3). [25] Thus, a small decrease in the free energy may be enough for intra-molecular gating rearrangements to activate TRPV1. However, even if several short little hairpin stems were included, such a small decrease may be insufficient to produce a high Q_{10} for noxious heat detection. Therefore, a decrease in the total minimum loop sizes of little hairpins to control the decrease in all the non-covalent interactions and the increase in heat capacity along the gating pathway should be considered. In agreement with this proposal, when the total number of all minimum hairpin sizes dramatically decreased from 121 to 97 residues in the loops upon the decrease of the total non-covalent interactions from 77 to 67, the resultant structural thermo-sensitivity (Ω_{10}) was comparable to the functional thermo-sensitivity (Q_{10}). For PI-free rTRPV1, the calculated Ω_{10} was about 20.7 while the experimental Q_{10} is about 16.4. For PI-bound rTRPV1, the predicted Ω_{10} was about 26.1 while the experimental Q_{10} is in a range from 21.9 to 26. [1, 14] A little high Ω_{10} values in both cases may be due to a tight interaction between rTRPV1 and MSP2N2. [14] However, the presence of the PI lipid at the vanilloid site apparently increased both Ω_{10} and Q_{10} values by about 1/3. [14] When the intensity of a non-covalent interaction ranged from the minimal 0.5 kJ/mol to the maximal 3 kJ/mol, the normal Ω_{10} could be 11.4-96.4 (**Table 1**). Therefore, any measured Q_{10} values may be reasonable in this range.

Since a decrease in the total minimum loop sizes of little hairpins upon a decrease in the total non-covalent interactions along the gating pathway may be responsible for heat-evoked channel opening from a closed state and the related high Q_{10}, in addition to the biggest little

hairpins to start the temperature threshold of TRPV1, the third biggest little hairpin and other smaller little hairpins may play different roles.

The third biggest little hairpin had a minimum 12-residue loop from R557 to E570 to stabilize the open state of the TRPV1 (Fig. 3, 6). As the mutation R557E/A/L or E570L/A can disrupt the stimulatory R557-E570 H-bond, it is reasonable that the R557E or E570L mutant leads to a complete loss of function, or mutants R557A/L and E570A have low heat sensitivity, or E570A increases the threshold from 41.5°C to 44.3°C. [26, 27]

The first smaller little hairpin had no residue in the loop from Y441 and though F516 and Y554 and Y555 and back to Y441. It was shared by both closed and open states (Figs 2-3), and the related aromatic residues were highly conserved in thermosensitive TRPV1-4 but not in non-thermosensitive TRPV5-6. [28] The tight π interactions may allow it to serve as a relatively stationary anchor against which the S4–S5 linker can uplift in favor of TRPV1 opening. In support of this notion, the Y441S, Y444S, Y554A or Y555S mutation leaves the channel not functional. [26, 29]

The second smaller little hairpin had a minimum 6-residue loop from D576 to K579 and F580 and L678 and T685 via the D576-T685 and D576-R579 H-bonds and the F580-L678 CH-π interaction (**Figs. 1, 2, 4, 5**). The D576-R579 H-bond was disrupted in the open state (**Fig. 3**). It has been reported that the mutant R579E is not functional and the D576N/R or R579A mutant is less sensitive to heat than wild type rTRPV1. [26] Since the residues for this smaller little hairpin are conserved in TRPV1-6, it may serve as a key common anchor in the pore domain. [28]

The third smaller little hairpin had no residue in the loop from Y584 to T641 and F640 and Y666 and back to Y584. The residues for this smallest hairpin were also highly conserved in TRPV1-4 but not in TRPV5-6. [28] In agreement with its importance, the Y666A mutation is not functional while the F640L or T641S mutation decreases the temperature threshold to allow them to be constitutively active at room temperature. [30-31]

The fourth smaller little hairpin had a minimum 7-residue loop from N628 to D601 and N652 and T650 and F649 and E636 to stabilize the open state (**Fig. 3A**). It has been reported that the N628K or N652T or Y653T or combined mutation increases the temperature threshold, and the triple mutant N628K/N652T/Y653T has the longer opening durations [7] Furthermore, the N628L greatly decreases the heat sensitivity (Q_{10}~2.6) but the N628D has the opposite effect (Q_{10}~86), [14] possibly by mediating the heat stablity of this smaller little hairpin. On the other

hand, the turret deletion or replacement with glycine between G603 and N626 in mouse TRPV1 (mTRPV1) decreases the temperature threshold to a different extent, [8] possibly by weakening the corresponding R410-D510 salt bridge in the VSLD/pre S1 interface or generating another new biggest little hairpin with a minimum size larger than 16 residues in the loop along the gating pathway from D389 to K711. Notebly, although the deletion of the turret (Δ604-626) still allows the TRPV1 mutant construct to be activated by heat, the binding of external double-knot toxin or vanillotoxin (DkTX) to the outer pore prevents heat activation, [9, 15] possibly by disrupting the N628-D601-N652 or Y584-T7641-Y666 H-bonding network.

The fifth smaller little hairpin had a minimum 1-residue loop linking W426 on pre-S1, F434 on S1, Y555 and R557 on S4, and Q700 and R701 together. This little hairpin topological structure was highly conserved in different gating states and thus may also act as a solid anchor upon which the S4–S5 linker can uplift to facilitate TRPV1 opening (**Figs. 1-6**). The sixth smaller little hairpin had no residue in the loop from Y401 to Q498 and R499 and back to Y401 to hold the high Q_{10} (**Figs. 3, 6**). The seventh smaller hairpin had no residue in the loop from Y444 to M445 to W549 to T449 and F448 and back to Y544. It was highly conserved in all the gating states and thus may serve as a static anchor (**Figs. 1-6**). Further experiments are necessary to test these possibilities.

4. CLOSING REMARK

The little hairpin topological loop structures can be used to design a thermosensitive bio-thermometer with a high Q_{10} value. In addition to the ionic strength in the physiological range, the little hairpin size and the number and the intensity of the hairpin-forming non-covalent interactions between amino acid side chains can be used to tune the little hairpin strength for different melting temperature thresholds to detect distinct small environmental temperature changes. These non-covalent interactions include salt bridges, aromatic side chain π interactions and H-bonds. Both the biggest and smaller little hairpins are necessary to control the temperature threshold and the thermal efficacy. Their opening and closure should be reversible and fast enough to have a very large effect on channel gating, which can be easily coupled to an electrical readout in the primary afferent sensor neuron. In this regard, this study may provide a broad structural basis for thermosensitive TRP channels to work as a bio-thermometer.

5. MATERIALS AND METHODS

In this *in silico* study, the little hairpin topological structural aspects of rTRPV1 channels below and above the temperature threshold were investigated and analyzed with graph theory as the bio-thermometer basis for noxious heat detection. The *in silico* protomer models were based on the cryo-EM structural data of closed rTRPV1 in MSP2N2 with PI-bound at 4°C (PDB ID, 7LP9, model resolution= 2.63 Å) and 48°C (PDB ID, 7LPC, model resolution= 3.07 Å), capsaicin-bound at 4°C (PDB ID, 7LPA, model resolution= 3.37 Å) and 25°C (PDB ID, 7LPB, model resolution= 3.54 Å) and 48°C (PDB ID, 7LPD, model resolution= 3.55 Å), open rTRPV1 with capsaicin-bound at 48°C (PDB ID, 7LPE, model resolution= 3.72 Å), [14] UCSF Chimera was used to assess non-covalent interactions in TRPV1. All the stereo- or regioselective diagonal and lateral non-covalent interactions such as salt-bridges and lone pair/CH/cation-π interactions and H-bonds between amino acid side chains along the gating pathway from D388 in the pre-S1 domain to K710 in the TRP domain of rTRPV1 were included to test their potential roles in forming the little hairpins with minimum loop sizes, controlling the temperature threshold and stablizing the heat afficacy for the higher temperature coefficient Q_{10}. The standard definition of non-covalent interactions was employed.

The minimum loop sizes in the little hairpin to control the non-covalent interactrions were calculated using graph theory. The primary amino acid sequence line from D388 to K710 was marked in black. An amino acid side chain involving a non-covalent interaction along the gating pathway of rTRPV1 was defined as a vertex and marked with an arrow in different colors. The same kind of non-covalent interactions between two amino acid side chains was marked in the same color for an edge. A hairpin topologicval loop was considered significant when an edge forms a sealed topological ring with the amino acid sequence between two ends of the edge or other edges. The minimum loop size L was definded as the number of residues that do not participate in any non-covalent interctions in the little hairpin loop. Only the minimum loop sizes of the little hairpins were marked in black. The biggest and smaller little hairpin sizes for channel gating were shown in red circles. The total number of all noncovalent interactions and minimum hairpin loop sizes along the gating pathway were shown in black and blue circles, respectively.

The temperature threshold was calculated from the melting temperature T_m of the biggest little hairpin along the gating pathway using the following equation: [17]

$$T_m\ (°C) = 34 + (n-2)\times 10 + (20-L_{max})\times 2$$

where, n is the total number of the non-covalent interactions equivalent to H-bonds in the biggest little hairpin, and L_{max} is the loop length of the biggest little hairpin.

If a thermosensitive ion channel changes from a closed state to an open state within a temperature range ΔT, $\Omega_{\Delta T}$ was used to evaluate the structural thermo-sensitivity of a single ion channel as calculated using the following equation:

$$\Omega_{\Delta T} = [(L_o - L_c)E/2]^{(Nc/No)}$$

where, L_o and L_c are the total numbers of all the minimum lengths of little hairpins along the gating pathway in the open and closed states, respectively; N_c and N_o are the total numbers of all the non-covalent interactions along the gating pathway in the closed and open states, respectively; E is the energy intensity of a non-covalent interaction in a range of 0.5-3 kJ/mol. Usually, E=1 kJ/mol.

When ΔT=10°C, Ω_{10} could be comparable to the functional thermo-sensitivity (Q_{10}) of a single ion channel. Q_{10} was calculated using the following equation:

$$Q_{10} = (R2/R1)^{10/(T2-T1)}$$

where, R1 and R2 are rates of a reaction at two different temperatures T1 and T2 in Celsius degrees or kelvin, respectively.

Conventions and Abbreviations: cryo-EM, cryo-electron microscopy; DkTx, double-knot toxin or vanillotoxin; PI, phosphatidylinositol; TRP, transient receptor potential; TRPV1, TRP vanilloid-1; TRPVi (i=1; 2, 3, 4, 5, 6); hTRPV1, human TRPV1; mTRPV1, mouse TRPV1; pTRPV1, platypus TRPV1; rTRPV1, rat TRPV1; VSLD, voltage-sensor-like domain

Acknowledgements

The author's own studies cited in this article were supported by NIDDK Grant (DK45880 to D.C.D.) and Cystic Fibrosis Foundation grant (DAWSON0210) and NIDDK grant (2R56DK056796-10) and American Heart Association (AHA) Grant (10SDG4120011 to GW).

Conflict of Interest: The author declares no conflict of interest.

Data Availability Section: This study includes no data deposited in external repositories

References

1. M. J. Caterina, M. A. Schumacher, M. Tominaga, T. A. Rosen, J. D. Levine, D. Julius. The capsaicin receptor: a heat-activated ion channel in the pain pathway. *Nature* **1997**, 389, 816.
2. J. B. Davis, J. Gray, M. J. Gunthorpe, J. P. Hatcher, P. T. Davey, P. Overend, M. H. Harries, J. Latcham, C. Clapham, K. Atkinson, S. A. Hughes, K. Rance, E. Grau, A. J. Harper, P. L. Pugh, D. C. Rogers, S. Bingham, A. Randall, S. A. Sheardown. Vanilloid receptor-1 is essential for inflammatory thermal hyperalgesia. *Nature* **2000**, 405,183.
3. N. R Gavva; J. J. S. Treanor, A. Garami, L. Fang, S. Surapaneni, A. Akrami, F. Alvarez, A. Bak, M. Darling, A. Gore, G. R. Jang, J. P. Kesslak, L.Ni, M. H. Norman, G. Palluconi, M. J. Rose, M. Salfi, E. Tan, A. A. Romanovsky, C. Banfield, G. Davar. Pharmacological blockade of the vanilloid receptor TRPV1 elicits marked hyperthermia in humans. *Pain* **2008**, 136, 202.
4. I. Vandewauw, K. De Clercq, M. Mulier, K. Held, S. Pinto, N. V. Ranst, A. Segal, T. Voet, R. Vennekens, K. Zimmermann, J. Vriens, T. Voets. A TRP channel trio mediates acute noxious heat sensing. *Nature* **2018**, 555, 662.
5. M. K. Chung, S. Wang. Cold suppresses agonist-induced activation of TRPV1. *J Dent Res* **2011**, 90, 1098.
6. S. E. Jordt, D. Julius. Molecular basis for species-specific sensitivity to “hot” chili peppers. *Cell* **2002**, 108, 421.
7. J. Grandl, S. E. Kim, V. Uzzell, B. Bursulaya, M. Petrus, M. Bandell, A. Patapoutian. Temperature-induced opening of TRPV1 ion channel is stabilized by the pore domain. *Nat Neurosci.* **2010**, 13, 708.
8. Y. Cui, F. Yang, X. Cao, V. Y. Yarovoy, K.W. Wang, J. Zheng. Selective disruption of high sensitivity heat activation but not capsaicin activation of TRPV1 channels by pore turret mutations. *J. Gen. Physiol.* **2012**, 139, 273.
9. A. Jara-Oseguera, C. Bae, K. J. Swartz. An external sodium ion binding site controls allosteric gating in TRPV1 channels. *Elife* **2016**, 5.
10. S. B. Long, E. B. Campbell, R. Mackinnon. Crystal structure of a mammalian voltage-dependent Shaker family K^+ channel. *Science* **2005**, 309, 897.

11. M. Liao, E. Cao, D. Julius, Y. Cheng. Structure of the TRPV1 ion channel determined by electron cryo-microscopy. *Nature* **2013**, 504,107.
12. E. Cao, M. Liao, Y. Cheng, D. Julius. TRPV1 structures in distinct conformations reveal activation mechanisms. *Nature* **2003**, 504, 113.
13. K. D. Nadezhdin, A. Neuberger, Y. A. Nikolaev, L. A. Murphy, E. O. Gracheva, S. N. Bagriantsev, A. I. Sobolevsky. Extracellular cap domain is an essential component of the TRPV1 gating mechanism. *Nat Commun.* **2021**, 12, 2154.
14. D. H. Kwon, F. Zhang, Y. Suo, J. Bouvette, M. J. Borgnia, S.-Y. Lee, Heat-dependent opening of TRPV1 in the presence of capsaicin. *Nat Struct Mol Biol*. **2021**, 28, 554.
15. Y. Gao, E. Cao, D. Julius, Y. Cheng. TRPV1 structures in nanodiscs reveal mechanisms of ligand and lipid action. *Nature* **2016**, 534, 347.
16. G. Wang. Lipid-dependent sequential allosteric activation of heat-sensing TRPV1 channels by anchor-stereoselective "hot" vanilloid compounds and analogs. *Biochem. Biophys. Rep*. **2000**, 28, 101109.
17. A. T. Jonstrup, J. Fredsøe, A. H. Andersen. DNA Hairpins as Temperature Switches, Thermometers and Ionic Detectors. *Sensors* **2013**, 13, 5937.
18. M. J. Caterina, T. A. Rosen, M. Tominaga, A. J Brake, D. Julius. A capsaicin-receptor homologue with a high threshold for noxious heat. *Nature* **1999**, 398,436.
19. M. J. Caterina, A. Leffler, A. B. Malmberg, W. J. Martin, J. Trafton, K. R. Petersen-Zeitz, M. Koltzenburg, A. I. Basbaum, D. Julius. Impaired nociception and pain sensation in mice lacking the capsaicin receptor. *Science* **2000**, 288, 306.
20. A. M. Peier, A. J. Reeve, D. A. Andersson, A. Moqrich, T. J. Earley, A. C. Hergarden, G. M. Story, S. Colley, J. B. Hogenesch, P. McIntyre, S. Bevan, A. Patapoutian. A heat-sensitive TRP channel expressed in keratinocytes. *Science*. **2002,** 296, 2046.
21. G. D. Smith, M. J. Gunthorpe, R. E. Kelsell, P. D. Hayes, P. Reilly, P. Facer, J. E. Wright, J. C. Jerman, J-P. Walhin, L. Ooi, J. Egerton, K. J. Charles, D. Smart, A. D. Randall, P. Anand, J. B. Davis. TRPV3 is a temperature-sensitive vanilloid receptor-like protein. *Nature* **2002**, 418, 186.
22. H. Xu, I. S. Ramsey, S. A. Kotecha, M. M. Moran, J. A. Chong, D. Lawson, P. Ge, J. Lilly, I. Silos-Santiago, Y. Xie, P. S. DiStefano, R. Curtis, D. E. Clapham. TRPV3 is a calcium-permeable temperature-sensitive cation channel. *Nature* **2002**, 418, 181.

23. M. K. Chung, H. Lee, M. J. Caterina. Warm temperatures activate TRPV4 in mouse 308 keratinocytes. *J. Biol. Chem*. **2003**, 278, 32037.
24. L. Luo, Y. Wang, B. Li, L. Xu, P. M. Kamau, J. Zheng, F. Yang, S. Yang, R. Lai. Molecular basis for heat desensitization of TRPV1 ion channels. *Nat Commun.* **2019,** 10, 2134. Correction in: *Nat Commun*. **2020;** 11, 1798.
25. S. E. Kiehna, M. L. Waters. Sequence dependence of β-hairpin structure: Comparison of a salt bridge and an aromatic interaction. *Protein Science* **2003**, 12, 2657.
26. S. Boukalova, L. Marsakova, J. Teisinger, V. Vlachova. Conserved residues within the putative S4–S5 region serve distinct functions among thermosensitive vanilloid transient receptor potential (TRPV) channels. *J. Biol. Chem*. **2010**, 285, 41455.
27. M. Kim, N. J. Sisco, J. K. Hilton, C. M. Montano, M. A. Castro, B. R. Cherry, M. Levitus, W. D. V. Horn. Evidence that the TRPV1 S1-S4 membrane domain contributes to thermosensing. *Nat Commun.* **2020**, 11, 4169.
28. K. D. Nadezhdin, A. Neuberger, Y. A. Trofimov , N. A. Krylov , V. Sinica, , N. Kupko, V. Vlachova , E. Zakharian , R. G. Efremov, A. I. Sobo-levsky. Structural mechanism of heat-induced opening of a temperature-sensitive TRP channel. *Nat. Struct. Mol. Biol***. 2021,** 28, 564–572.
29. S. Boukalova, J. Teisinger, & V. Vlachova, Protons stabilize the closed conformation of gain-of-function mutants of the TRPV1 channel. *Biochim. Biophys. Acta*. **2013,** 1833,520.
30. K. Susankova, R. Ettrich, L. Vyklicky, J. Teisinger, V. Vlachova. Contribution of the Putative Inner-Pore Region to the Gating of the Transient Receptor Potential Vanilloid Subtype1 Channel (TRPV1). *J. Neurosci.* **2007,** 27, 7578.
31. B. R. Myers, C. J. Bohlen, D. Julius. A yeast genetic screen reveals a critical role for the pore helix domain in TRP channel gating. *Neuron* **2008**, 58, 362.

Figure legends

Figure 1. **The little hairpin topological structural network along the gating pathway of PI-free rTRPV1 in the closed state at 4°C. A,** The little hairpin topological loop map. The cryo-EM structure of closed rTRPV1 with capsaicin bound at 4°C (PDB ID, 7LPA) was used for the model.[14] The pore domain, the S4-S5 linker, the TRP domain, the VSLD and the pre-S1 domain are indicated in black. Salt bridges, π interactions, and H-bonds between pairing amino acid side chains along the gating pathway from D388 to K710 are marked in purple, green, and orange, respectively. The minimum loop sizes in the little hairpins required to control the relevant non-covalent interactions are labeled in black. The total numbers of all minimum hairpin loop sizes and non-covalent interactions along the gating pathway are shown in the blue and black circles, respectively. **B.** The structure of the 1st biggest little hairpin with a minimum 24-residue loop in the VSLD to control the Y463-K535 H-bond. **C.** The sequence of the 1st biggest little hairpin with a minimum 24-residue loop. The Y463-K535 H-bond is marked in a blue box.

Figure 2. **The little hairpin topological structural network along the gating pathway of PI-free rTRPV1 in the closed state at 25°C. A,** The little hairpin topological loop map. The cryo-EM structure of closed rTRPV1 with capsaicin bound at 25°C (PDB ID, 7LPB) was used for the model.[14] The pore domain, the S4-S5 linker, the TRP domain, the VSLD and the pre-S1 domain are indicated in black. Salt bridges, π interactions, and H-bonds between pairing amino acid side chains along the gating pathway from D388 to K710 are marked in purple, green, and orange, respectively. The minimum loop sizes in the little hairpins required to control the relevant non-covalent interactions are labeled in black. The total numbers of all minimum hairpin loop sizes and non-covalent interactions along the gating pathway are shown in the blue and black circles, respectively. **B,** The structure of the little hairpin with a minimum 7-residue loop in the VSLD to control the Y463-K535 H-bond. **C.** The structure of the 2nd biggest little hairpin with a minimum 10-residue loop in the VSLD/pre-S1 interface to control the R409-D509 salt bridge. **D,** The sequences of two little hairpins with minimum 7- and 10-residue loops to control the Y463-K535 H-bond and the R409-D509 salt bridge in the blue boxes, respectively.

Figure 3. **The little hairpin topological structural network along the gating pathway of PI-free rTRPV1 in the open state at 48°C. A,** The little hairpin topological loop map. The cryo-EM structure of open rTRPV1 with capsaicin bound at 48°C (PDB ID, 7LPE) was used for the model.[14] The pore domain, the S4-S5 linker, the TRP domain, the VSLD and the pre-S1 domain are indicated in black. Salt bridges, π interactions, and H-bonds between pairing amino acid side chains along the gating pathway from D388 to K710 are marked in purple, green, and orange, respectively. The minimum loop sizes in the little hairpins required to control the relevant non-covalent interactions are labeled in black. The total numbers of all minimum hairpin loop sizes and non-covalent interactions along the gating pathway are shown in the blue and black circles, respectively. **B,** The structure of the little hairpin with no residue in the loop in the VSLD/pre-S1 interface to disrupt the R409-D509 salt bridge. **C.** The structure of the 3rd biggest little hairpin with a minimum 12-residue loop in the VSLD/S4-S5 linker interface to control the stimulatory R557-E570 H-bonds and salt bridge. **D,** The sequences of two little hairpins with minimum 0- and 12-residue loops to control the Y401-Q498/R499 bridges and the R557-E570 bridge in the blue boxes, respectively.

Figure 4. **The little hairpin topological structural network along the gating pathway of PI-free rTRPV1 in the desensitized state at 48°C. A,** The little hairpin topological loop map. The cryo-EM structure of inactivated rTRPV1 with capsaicin bound at 48°C (PDB ID, 7LPD) was used for the model.[14] The pore domain, the S4-S5 linker, the TRP domain, the VSLD and the pre-S1 domain are indicated in black. Salt bridges, π interactions, and H-bonds between pairing amino acid side chains along the gating pathway from D388 to K710 are marked in purple, green, and orange, respectively. The minimum loop sizes in the little hairpins required to control the relevant non-covalent interactions are labeled in black. The total numbers of all minimum hairpin loop sizes and non-covalent interactions along the gating pathway are shown in the blue and black circles, respectively. **B,** The structure of the little hairpin with no residue in the loop in the VSLD/S4-S5 linker/TRP/VSLD interfaces to govern the R557-E570-Q700 H-bond network. **C.** The structure of the 4th biggest little hairpin with a minimum 7-residue loop in the VSLD to control the R455-Y537 H-bond for the inactivated state. **D,** The sequences of two little hairpins with minimum 0- and 7-residue loops to control the R557-E570-Q700 H-bond network and the R455-Y537 H-bond in the blue rectangles, respectively.

Figure 5. **The little hairpin topological structural network along the gating pathway of PI-bound rTRPV1 in the closed state at 48°C. A,** The little hairpin topological loop map. The cryo-EM structure of closed rTRPV1 with PI bound at 48°C (PDB ID, 7LPC) was used for the model.[14] The pore domain, the S4-S5 linker, the TRP domain, the VSLD and the pre-S1 domain are indicated in black. Salt bridges, π interactions, and H-bonds between pairing amino acid side chains along the gating pathway from D388 to K710 are marked in purple, green, and orange, respectively. The minimum loop sizes in the little hairpins required to control the relevant non-covalent interactions are labeled in black. The total numbers of all minimum hairpin loop sizes and non-covalent interactions along the gating pathway are shown in the blue and black circles, respectively. The dashed lines are absent in the native lipid system. The putative biggest little hairpin loop size in the native lipid system is labled in grey. **B,** The structure of the PI pocket. **C,** The structure of the 5th biggest little hairpin with a minimum 16-residue loop in the VSLD/pre-S1 interface to control the D509-R409 salt bridge near PI. **D,** The structure of the 6th biggest little hairpin with a minimum 12-residue loop in the VSLD to control the D509-PI-R557 bridge. **E,** The sequences of the 5th and 6th biggest little hairpins with minimum 12- and 16-residue loops to control the R557-PI-D509 bridge and the D509-R409 salt bridge in the blue rectangles, respectively.

Figure 6. The tentative model for TRPV1 opening and desensitization upon the heat-eveked melting of the biggest little hairpin. A. The cryo-EM structures of rTRPV1 in the closed and open and desensitized states (PDB ID: 7LPC, 7LPE, 7LPD, respectively) were used for the model. [14] In the presence of PI at the capsaicin site, rTRPV1 is closed below the threshold 42°C and has the biggest little hairpin with a minimum 16-residue loop and two equivalent H-bonds (red) to control the VSLD/pre-S1 interface. When the temperature increases above the threshold 42^0C, rTRPV1 is open upon the decrease of the minimum hairpin size from 16 residues to 0 in the loops in the VSLD/pre-S1 interface. In the meantime, the biggest little hairpin with a minimum 12-residue loop and 2 equivalent H-bonds (red) is formed in the VSLD/S4-S5 linker for the open state. However, in the desensitized state, rTRPV1 further inactivates with the presence of the fourth biggest little hairpin with a minimum 7-residue loop to control the interface between the S1-S2 linker and the S3-S4 linker in the temperature range from 42°C to 60°C . **B.** The proposed smaller

little hairpins for TRPV1 gating. The minimum loop sizes in little hairpins are shown in the red circles.

Figures

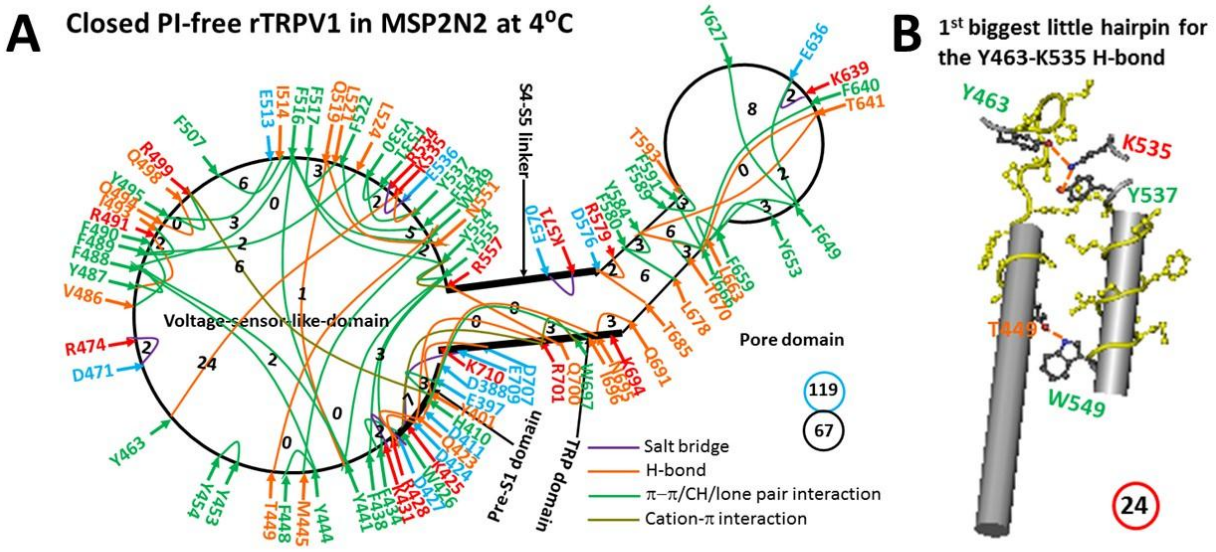

C 1st biggest little hairpin sequence : ^{449}TAAAYYRPVEGLPPY^{463}—^{535}K—^{537}YVASMVFSLAMGW^{549}—^{449}T

Figure 1

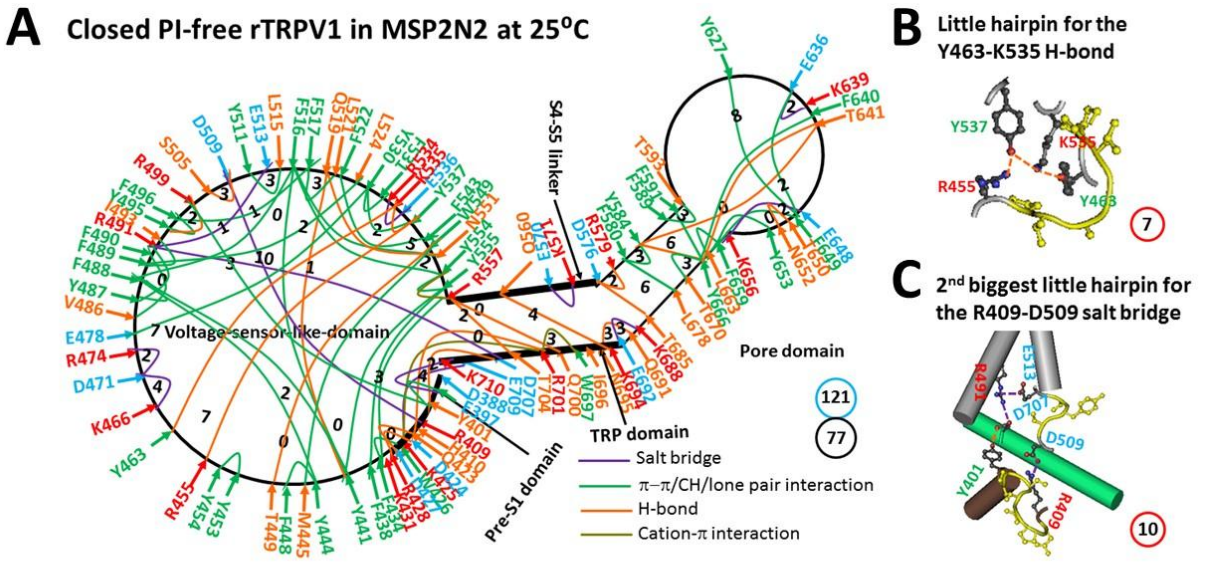

D Little hairpin sequence : ^{455}RPVEGLPPY^{463}—^{535}K—^{537}Y—^{455}R

2nd biggest little hairpin sequence : ^{401}YSSSETPNR^{409}—^{509}DSYSE^{513}—R^{491}—D^{707}—^{401}Y

Figure 2

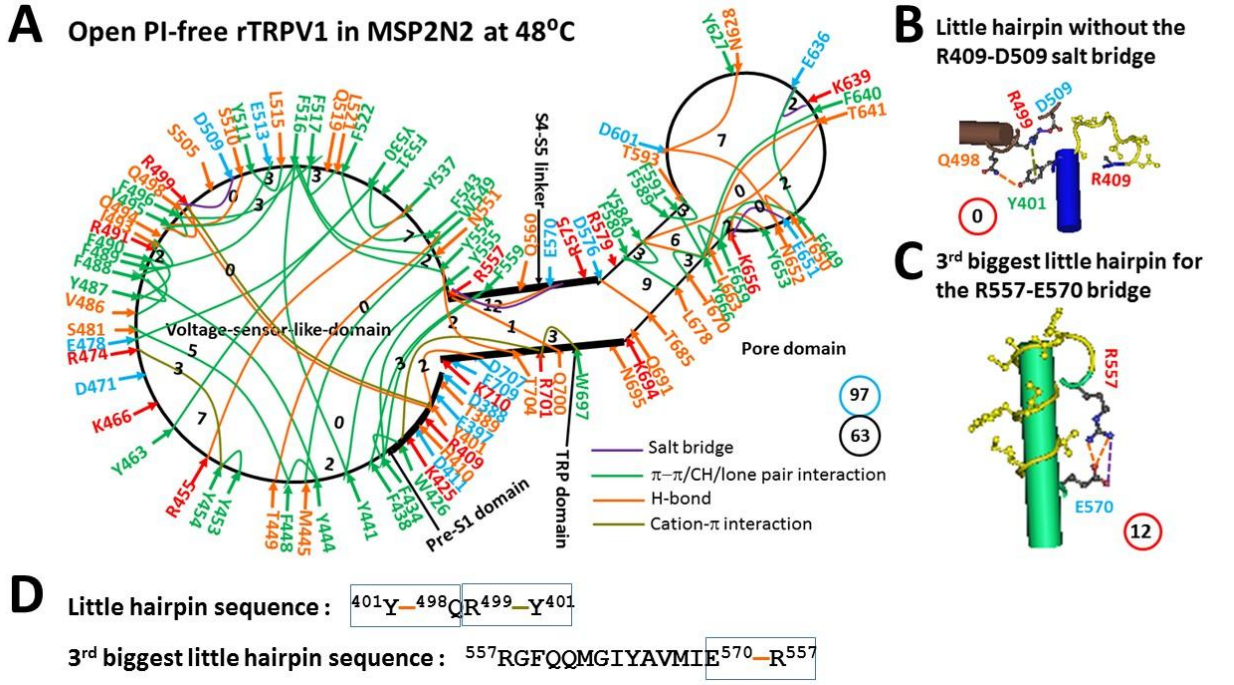

Figure 3

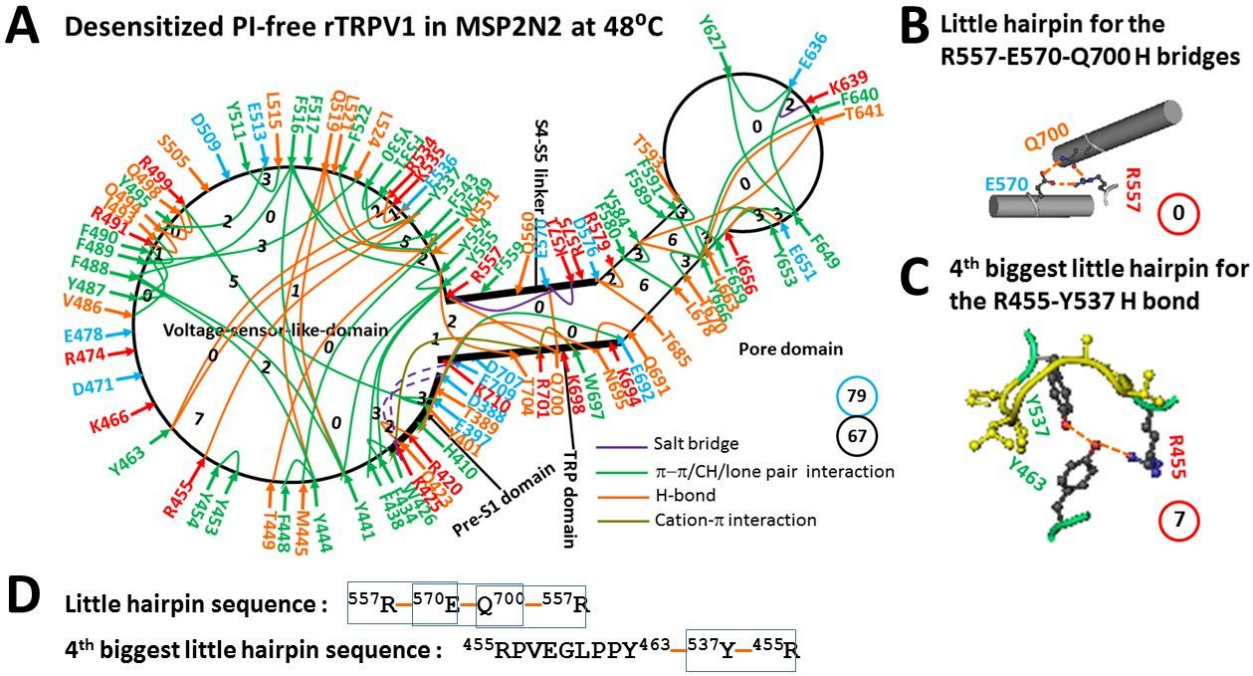

Figure 4

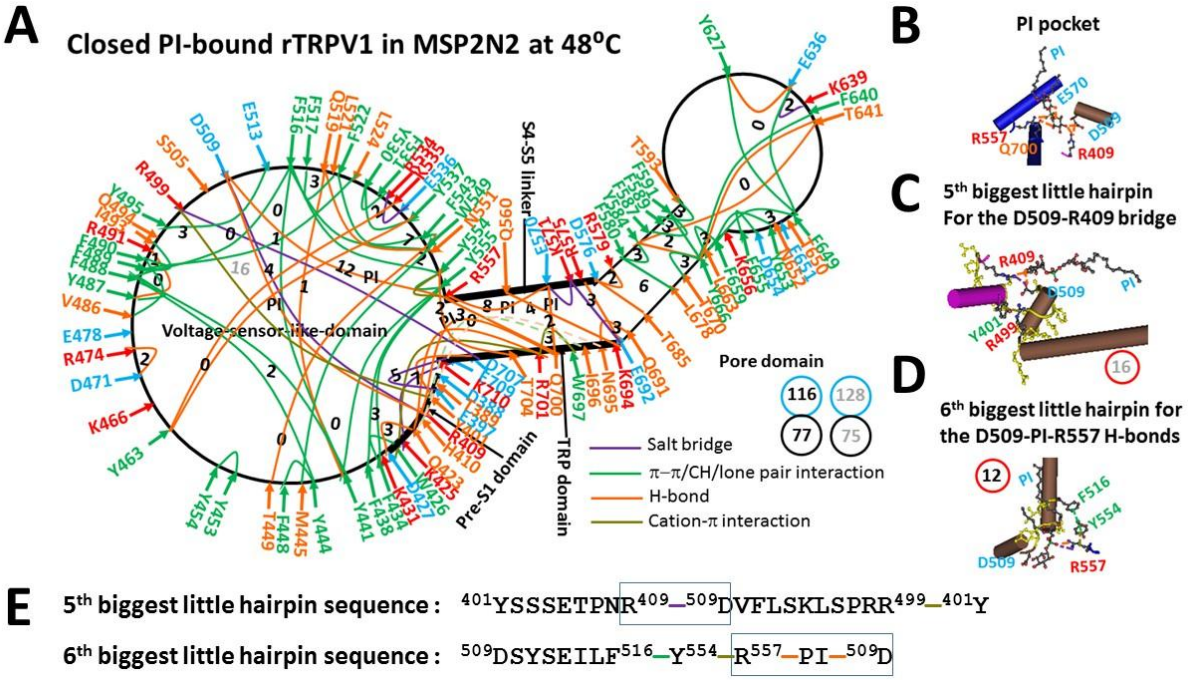

Figure 5

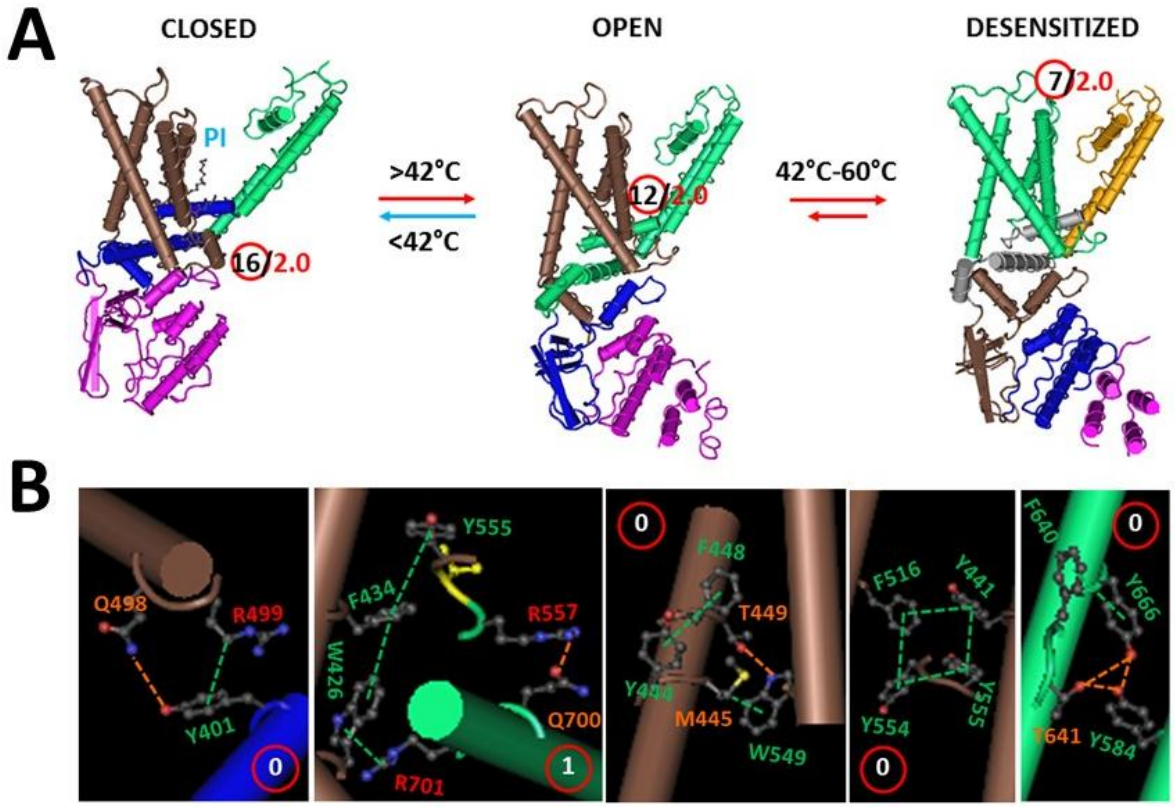

Figure 6